

Chapter 6

Magnetism of Itinerant Electrons



In insulators, the following picture is expected to describe the magnetism: the spins localized at the lattice point cause magnetism through various spin-to-spin interactions. Common ferromagnetic metals like iron, cobalt, and nickel are supposed to have largely different mechanism from the above. Namely, electrons migrating in crystals (itinerant electrons) have their spins aligned partially due to the correlation effect, which phenomenon may generate the ferromagnetism. When the correlation effect is not very strong and the system is paramagnetic, such itinerant electron systems can be treated within the Landau's Fermi liquid theory[1] as mentioned in Ch. 3. On the other hand, the correlation is so strong that a ferromagnetism appears, the difficulties in theories increase largely. It was not easy for theoretical models to explain such types of ferromagnetism to the level in which the theories can be comparable with experiments. Including such difficulties, we would like to review the present understandings and open questions in the last three weeks.

6.1 Hartree-Fock approximation of electron gas

We would have a brief look at the difficulty to have a realistic ferromagnetism in the model of electron gas. We use the simplest Hartree-Fock approximation (not very simple actually) of electron correlation.

6.1.1 Hartree-Fock approximation

Though you are already familiar with **Hartree-Fock (HF) approximation**, we will shortly review it here (we will not use such details in analysis of electron gas here). We consider an N -particle system, in which the particles occupy single-particle wavefunctions

$$\varphi_{k_1}, \varphi_{k_2}, \dots, \varphi_{k_N}. \quad (6.1)$$

The many body state of this N -body system can be expressed by the Slater determinant:

$$\Phi = \frac{1}{\sqrt{N!}} \begin{vmatrix} \varphi_{k_1}(x_1) & \cdots & \varphi_{k_N}(x_1) \\ \vdots & \ddots & \vdots \\ \varphi_{k_1}(x_N) & \cdots & \varphi_{k_N}(x_N) \end{vmatrix}, \quad (6.2)$$

which satisfies the fermion particle exchange statistics. x_i is a general coordinate, which contains all of single particle freedoms. We write the Hamiltonian in the form

$$\mathcal{H} = \sum_{j=1}^N h(x_j) + \sum_{\langle i,j \rangle} v(x_i, x_j), \quad (6.3)$$

where h is a single-particle Hamiltonian, v is a two-body interaction. In the HF approximation, we calculate the expectation value

$$\mathcal{W} = \langle \Phi | \mathcal{H} | \Phi \rangle, \quad (6.4)$$

and look for the set $\{\varphi_{k_j}\}$ that minimize \mathcal{W} with a variational method.

Here we use the ket representation $|k_j\rangle$ for φ_{k_j} . We assume the orthonormal basis condition:

$$\langle k_i | k_j \rangle = \delta_{ij}. \quad (6.5)$$

In this representation, \mathcal{W} is written as

$$\mathcal{W} = \sum_{j=1}^N \langle k_j | h | k_j \rangle + \sum_{\langle i,j \rangle} [\langle k_i k_j | v | k_i k_j \rangle - \langle k_i k_j | v | k_j k_i \rangle]. \quad (6.6)$$

In the rhs, in the term $\langle k_i k_j | v | k_i k_j \rangle$, the two particles interact in the same order but in $\langle k_i k_j | v | k_j k_i \rangle$, the two particles exchange their positions during the interaction. The former is called the direct integral, the latter is called the exchange integral (exchange interaction). In the following, we adopt the Lagrange multiplier method to minimize the energy of the system (6.6) under the constraint of (6.5). That is, we consider the quantity

$$\mathcal{W} - \sum_{\langle i,j \rangle} \lambda_{ij} \langle k_i | k_j \rangle, \quad (6.7)$$

which should be minimized. In order for that, we consider the condition that the variations of the above quantity with $\{\varphi_{k_j}^*\}$ are zero, which can be expressed as

$$h\varphi_{k_j} + \sum_{i=1}^N [\langle k_i | v | k_i \rangle \varphi_{k_j} - \langle k_i | v | k_j \rangle \varphi_{k_i}] = \sum_{i=1}^N \lambda_{ij} \varphi_{k_i}. \quad (6.8)$$

Here we define a single-body density matrix as

$$\rho(x, x') = \sum_{i=1}^N \varphi_{k_i}^*(x) \varphi_{k_i}(x'), \quad (6.9)$$

with which we further define v_{eff} and A as

$$v_{\text{eff}}(x) = \int dx' v(x, x') \rho(x', x'), \quad A(x) \varphi(x) = \int dx' v(x, x') \varphi(x') \rho(x', x). \quad (6.10)$$

Then eq. (6.8) is written as

$$[h(x) + v_{\text{eff}}(x) - A(x)] \varphi_{k_j}(x) = \sum_{i=1}^N \lambda_{ij} \varphi_{k_i}(x). \quad (6.11)$$

In eq. (6.11), the Hermite operator given in $[\dots]$ in the left hand side does not depend on the specific selection of k_j in the operand. Also the eigenfunctions are orthogonal to each other. Hence by taking φ_{k_j} as the eigenfunctions, we can write

$$[h(x) + v_{\text{eff}}(x) - A(x)] \varphi_{k_j}(x) = \epsilon_{k_j} \varphi_{k_j}(x). \quad (6.12)$$

Then we take N solutions in the ascending order from the lowest $\{\epsilon_{k_j}\}$. The Slater determinant of these N solutions is the ground state in the HF approximation. However, the operator in the $[\dots]$ part also depends on $\{\epsilon_{k_j}\}$ (though not depends on specific selection of the operand), (6.12) should be solved self-consistently. Equation (6.12) is called **Hartree-Fock equation**. This is essentially the same as the self-consistent equation in the molecular field approximation of the Heisenberg model. To see how to proceed the calculation in more specific physical problems, or how to go beyond the HF approximation (e.g., taking the effect of higher order term into account), refer to textbooks on many-body problems (e.g., [2, 3, 4]).

6.1.2 Jellium model and ferromagnetism

Here we adopt **jellium model**, in which the lattice potential is approximated by a uniform background with a plus charge. And we consider a free electron system in the background. The ground state in the absence of electron mutual interaction is the state in which the Fermi sphere is filled up as

$$|\Psi\rangle = \prod_{E(\mathbf{k},\sigma) \leq E_F} c_{\mathbf{k}\sigma}^\dagger |0\rangle. \quad (6.13)$$

Next we write down the Hamiltonian in the presence of electron-electron interaction as

$$\mathcal{H} = \sum_{\mathbf{k},\sigma} \epsilon_{\mathbf{k}} c_{\mathbf{k}\sigma}^\dagger c_{\mathbf{k}\sigma} + \frac{1}{2V} \sum_{\mathbf{k},\mathbf{k}',\sigma,\sigma',\mathbf{q} \neq 0} v_{\mathbf{q}} c_{\mathbf{k}+\mathbf{q},\sigma}^\dagger c_{\mathbf{k}'-\mathbf{q},\sigma'}^\dagger c_{\mathbf{k}'\sigma} c_{\mathbf{k}\sigma}, \quad (6.14)$$

where V is the system volume, $\epsilon_{\mathbf{k}} = \hbar^2 k^2 / 2m$ and $v_{\mathbf{q}} = 4\pi e^2 / q^2$. The Fermi wavenumber k_F is determined from the Fermi energy E_F , and the only parameter that characterizes the system is the averaged electron distance measured by Bohr radius a_B :

$$r_s \equiv \frac{1}{a_B} \left[\frac{3}{4\pi(k_F^3/3\pi^2)} \right]^{1/3}, \quad (6.15)$$

in the jellium model.

Because the system has spatially translational symmetry in the jellium model, plane waves are already the solutions of self-consistent HF equation (6.12), and then the residual procedure of the HF approximation is to minimize the energy of many-body state. The kinetic energy per single electron is

$$\epsilon_{ke} = \frac{1}{N} \sum_{\mathbf{k}s} \epsilon_{\mathbf{k}} n_{\mathbf{k}s} = \frac{2V}{N} \int \frac{d^3k}{(2\pi)^3} \frac{\hbar^2 k^2}{2m} n_{\mathbf{k}} = \frac{3}{10} \frac{\hbar^2 k_F^2}{m} = \frac{2.21}{r_s^2} \text{Ry}, \quad (6.16)$$

where $\text{Ry} = \hbar^2 / 2ma_B^2 = 13.6 \text{ eV}$ is the unit named ‘‘Rydberg,’’ and is the binding energy of hydrogen atom. The Hartree term that corresponds to the direct integral is vanished by the charge neutral condition of jellium model. The exchange term, that is the expectation value of interaction between the states of exchanged particles. It is then

$$\epsilon_{ex} = -\frac{1}{2NV} \sum_{\mathbf{k},\mathbf{q} \neq 0,s} v_{\mathbf{q}} \langle \psi | c_{\mathbf{k}+\mathbf{q},s} c_{\mathbf{k}+\mathbf{q},s}^\dagger c_{\mathbf{k}s} c_{\mathbf{k}s} | \psi \rangle = \frac{1}{2NV} \sum_{\mathbf{k}s} v_{\mathbf{q}} n_{\mathbf{k}+\mathbf{q}} n_{\mathbf{k}}, \quad (6.17)$$

per an electron. The summation can be carried out as an integral over \mathbf{q} to be

$$\epsilon_{ex} = -\frac{3e^2}{4} \frac{k_F}{\pi} = -\frac{0.92}{r_s} \text{Ry}. \quad (6.18)$$

Then the total Hartree-Fock energy is

$$\epsilon_{hf} = \left(\frac{2.21}{r_s^2} - \frac{0.92}{r_s} \right) \text{Ry}. \quad (6.19)$$

From eq. (6.16), the total kinetic energy of electrons per unit volume is

$$E_{ke} = \frac{3}{10} \frac{\hbar^2 k_F^2}{m} \frac{4\pi}{3} \left(\frac{k_F}{2\pi} \right)^3 = \frac{\hbar^2 k_F^5}{20\pi^2 m}. \quad (6.20)$$

Let $(k_{F\uparrow}, n_{\uparrow}), (k_{F\downarrow}, n_{\downarrow})$ be the Fermi wavenumber and the electron number of up and down spin states respectively. Then

$$E_{\text{ke}}(p) = \frac{\hbar^2}{20\pi^2 m} (k_{F\uparrow}^5 + k_{F\downarrow}^5) = \frac{3(6\pi^2)^{2/3} \hbar^2}{10m} (n_{\uparrow}^{5/3} + n_{\downarrow}^{5/3}) = \frac{3(6\pi^2)^{2/3} \hbar^2}{10m} [p^{5/3} - (1-p)^{5/3}] n_0^{5/3}, \quad (6.21)$$

$$E_{\text{ex}}(p) = -\frac{3e^2}{4} \left(\frac{6}{\pi}\right)^{1/3} (n_{\uparrow}^{4/3} + n_{\downarrow}^{4/3}) = -\frac{3e^2}{4} \left(\frac{6}{\pi}\right)^{1/3} [p^{4/3} - (1-p)^{4/3}] n_0^{4/3}. \quad (6.22)$$

Here because polarization $0.5 \leq p \leq 1$ is defined as $n_{\uparrow} = pn_0, n_{\downarrow} = (1-p)n_0, p = 1$ corresponds to perfect polarization, $p = 0.5$ corresponds to no polarization. Then let ΔE be

$$\Delta E = [E_{\text{ke}}(1) + E_{\text{ex}}(1)] - [E_{\text{ke}}(0.5) + E_{\text{ex}}(0.5)], \quad (6.23)$$

then if $\Delta E < 0$, the ground state is a spin-polarized ferromagnetic state. This condition can be calculated from the above and expressed with the average distance parameter defined in eq. (6.15), as

$$r_s > 5.4531. \quad (6.24)$$

However, we found several ordinary metals with $r_s \sim 5$. Hence the above criterion does not fit the reality.

6.1.3 Electron correlation

The above discrepancy should come from either overestimation of lowering in the Coulomb energy with avoiding each other between parallel spins, or that of the Coulomb repulsion energy between antiparallel spins. The latter seems to be more plausible because the itinerant electrons with antiparallel spins also should avoid each other to lower the Coulomb repulsion energy. That means, in the jellium model, the solution of antiparallel spins in HF (mean field) approximation is not good enough for discussion of ground state. We need to go for higher order approximation or to consider some different approximation. We here define **correlation energy** as the energy difference between the energy of true ground state and that of mean field approximation.

There exist various methods in the estimation of correlation energy. Figure 6.1 shows a phase diagram of charged fermion gas in the jellium model calculated by diffusion Monte-Carlo method[5]. The red line indicates spin-polarized gas and the ferromagnetism appears in the region that the red line lies below the blue broken line which indicates unpolarized gas. However as can be seen, r_s for the appearance of the ferromagnetism is around 70, which is too sparse for real metals. Around $r_s \sim 90$ the Wigner crystal in which the electrons form a crystal and localize. This means if the correlation energy is correctly estimated, the ferromagnetism in common metallic ferromagnet like iron or nickel cannot be explained at all.

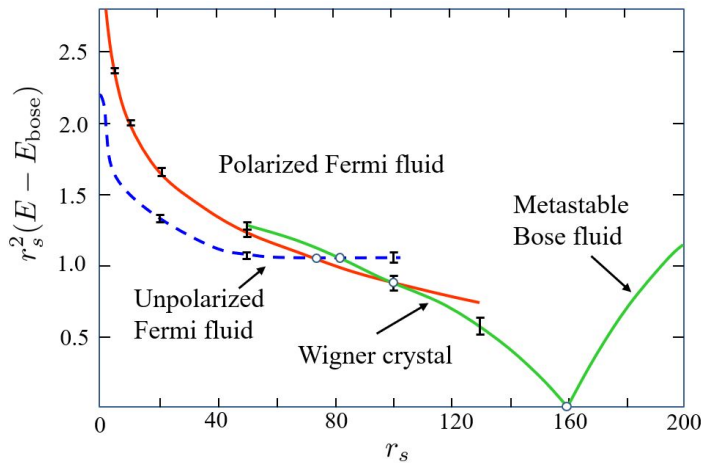


Fig. 6.1 Phase diagram of electron gas calculated by diffusion Monte-Carlo method. The energy origin (0) is taken to that of a bosonic system. The region where the red line lies lowest position should be ferromagnetic. From [5].

6.2 HF approximation in Hubbard model

The jellium model, not only in the mean field approximation, even with correct estimation of correlation energy, is far from the realistic explanation of ferromagnetism in metals. In the case of ferromagnets caused by double-exchange interaction, which we have seen in the previous chapter, the electrons hopping between local sites mediate ferromagnetic interaction between localized spins. Though the situation is different in the case of $3d$ transition metals, it can be a hint that the coexistence of localization and hopping can cause ferromagnetism in realistic conditions. Then we try to consider the Hubbard model introduced in Sec. 4.1.3.

6.2.1 Hubbard model for multiple site

We introduced two-site Hubbard model (sometimes referred to as Kanamori-Hubbard model) in Sec. 4.1.3. It is expected to describe from insulators, metals, ferromagnets and superconductors in spite of its compactness, and has been long used in theories. As we saw there, the long range part of the Coulomb interaction is ignored and the Coulomb repulsion only works between electrons in the same site (on-site interaction). On the other hand, the electrons hop between site i and site j with probability t_{ij} . The Hamiltonian for a general number of sites is

Hubbard Hamiltonian (1)

$$\mathcal{H} = \sum_{i,j,s} t_{ij} c_{is}^\dagger c_{js} + U \sum_i \hat{n}_{i\uparrow} \hat{n}_{i\downarrow}, \quad (6.25)$$

where s is the spin freedom. c_{is} satisfies the fermion commutation relation

$$\{c_{is}^\dagger, c_{is'}\} = \delta_{ij} \delta_{ss'}. \quad (6.26)$$

In the first hopping term, the annihilation operator c_{is} and hopping transition matrix element t_{ij} are Fourier-expanded as

$$c_{is} = \frac{1}{\sqrt{N}} \sum_{\mathbf{k}} e^{i\mathbf{R}_i \cdot \mathbf{k}} a_{\mathbf{k}s}, \quad t_{ij} = \frac{1}{N} \sum_{\mathbf{k}} \epsilon_{\mathbf{k}} e^{i\mathbf{k} \cdot (\mathbf{R}_i - \mathbf{R}_j)}. \quad (6.27)$$

\mathbf{R}_i is the spatial coordinate of site i . With substituting these into the first term in the right hand side of (6.25), because

$$\sum_{\langle i,j \rangle, s} t_{ij} c_{is}^\dagger c_{js} = \sum_{i,j,s} \frac{2}{N^2} \sum_{\mathbf{k}_1, \mathbf{k}_2, \mathbf{k}_3} \epsilon_{\mathbf{k}_1} e^{i\mathbf{k}_1 \cdot (\mathbf{R}_i - \mathbf{R}_j)} e^{-i\mathbf{k}_2 \cdot \mathbf{R}_i} a_{\mathbf{k}_2 s}^\dagger e^{i\mathbf{k}_3 \cdot \mathbf{R}_j} a_{\mathbf{k}_3 s} = \sum_{\mathbf{k}, s} \epsilon_{\mathbf{k}} a_{\mathbf{k}s}^\dagger a_{\mathbf{k}s}, \quad (6.28)$$

we can view the hopping (1st) term as kinetic energy term of wide-spreading electrons. From this, (6.25) can be expressed as follows.

$$\mathcal{H} = \sum_{\mathbf{k}, s} \epsilon_{\mathbf{k}} a_{\mathbf{k}s}^\dagger a_{\mathbf{k}s} + U \sum_i \hat{n}_{i\uparrow} \hat{n}_{i\downarrow}. \quad (6.29)$$

The Hubbard model is widely used in the study of many-body problem. Particularly it is practical to be applied to the ferromagnetism of $3d$ transition metals. In such systems, $4s$ and $3d$ electrons coexist in single band. $3d$ electrons are the origin of ferromagnetism and though the wavefunctions spread over the whole crystal (itinerant) they have high probabilities of existence at atomic positions, i.e. tendency to localize. On the other hand, $4s$ electrons tend to delocalize and screen the Coulomb interaction between $3d$ electrons. This property justifies the approximation of on-site short range Coulomb interaction.

6.2.2 HF approximation

We apply HF (mean field, molecular field) approximation to the Hubbard model. There is the same problem of overestimation as that in electron gas, but we will see what is different in the case of Hubbard model.

To estimate the ferromagnetic transition, we consider magnetization and electron number per site:

$$m = \langle n_{\uparrow} \rangle - \langle n_{\downarrow} \rangle, \quad n = \langle n_{\uparrow} \rangle + \langle n_{\downarrow} \rangle, \quad (6.30)$$

and compare the expectation values of energy for the states of $m = 0$ and $m \neq 0$. The magnetization is expressed in the unit of μ_B and g -factor is set to 2.

In the HF approximation of Hubbard model (6.25), the second term (interaction term) is simplified as

$$\begin{aligned} U \sum_i \hat{n}_{i\uparrow} \hat{n}_{i\downarrow} &= U \sum_i [\langle \hat{n}_{\uparrow} \rangle \hat{n}_{i\downarrow} + \langle \hat{n}_{\downarrow} \rangle \hat{n}_{i\uparrow} - \langle \hat{n}_{\uparrow} \rangle \langle \hat{n}_{\downarrow} \rangle + (\hat{n}_{i\uparrow} - \langle n_{\uparrow} \rangle)(\hat{n}_{i\downarrow} - \langle n_{\downarrow} \rangle)] \\ &\simeq U \sum_i (\langle \hat{n}_{\uparrow} \rangle \hat{n}_{i\downarrow} + \langle \hat{n}_{\downarrow} \rangle \hat{n}_{i\uparrow}) - NU \langle n_{\uparrow} \rangle \langle n_{\downarrow} \rangle \end{aligned} \quad (6.31)$$

$$\text{Take average} \rightarrow = \frac{NU}{4}(n^2 - m^2). \quad (6.32)$$

Namely, the second order term of fluctuation $(\hat{n}_{i\uparrow} - \langle n_{\uparrow} \rangle)(\hat{n}_{i\downarrow} - \langle n_{\downarrow} \rangle)$ is ignored. In this approximation, \downarrow -electrons work as an average on an \uparrow -electron, conversely, \uparrow -electrons work as an average on a \downarrow -electron. The last equation shows the expectation value for eigenstates.

We can rewrite eq. (6.31) with the Fourier expansions in (6.27), (6.28) to a Hamiltonian with the operators $\hat{n}_{\mathbf{k}s}$ as

$$\mathcal{H}_{\text{HF}} = \sum_{\mathbf{k},s} (\epsilon_{\mathbf{k}} + U \langle n_{-s} \rangle) n_{\mathbf{k}s} - NU \langle n_{\uparrow} \rangle \langle n_{\downarrow} \rangle. \quad (6.33)$$

Here we assign $s = \pm 1$ to spin \uparrow, \downarrow , and use the relation

$$\langle n_s \rangle = \frac{1}{2}(n + sm), \quad (6.34)$$

to obtain

$$\begin{aligned} \mathcal{H}_{\text{HF}} &= \sum_{\mathbf{k},s} \left(\epsilon_{\mathbf{k}} - \frac{sUm}{2} \right) \hat{n}_{\mathbf{k}s} + \frac{NU}{4}(n^2 + m^2) \\ &\equiv \sum_{\mathbf{k},s} \tilde{\epsilon}_{\mathbf{k}s} \hat{n}_{\mathbf{k}s} + \frac{NU}{4}(n^2 + m^2), \end{aligned} \quad (6.35)$$

where we take averages as $\sum_{\mathbf{k},s} \hat{n}_{\mathbf{k}s} \rightarrow N(\langle n_{\uparrow} \rangle + \langle n_{\downarrow} \rangle)$. That is, the appearance of the magnetization m shifts the single electron energy by $\Delta\mu = (-s)Um/2$. The directions of the shifts are opposite depending on spins. With packing the electrons into this band up to a common chemical potential μ , the total energy is given by

$$\begin{aligned} E &= \sum_{\tilde{\epsilon}_{\mathbf{k}s} \leq \mu} \left(\epsilon_{\mathbf{k}} - \frac{sUm}{2} \right) + \frac{NU}{4}(n^2 + m^2) \\ &= \sum_{\tilde{\epsilon}_{\mathbf{k}s} \leq \mu} \epsilon_{\mathbf{k}} + \frac{NU}{4}(n^2 - m^2). \end{aligned} \quad (6.36)$$

On the other hand, the spin-dependence of $\Delta\mu$ brings about the difference in the electron numbers in \uparrow and \downarrow states. And the difference should be equal to m . This is the **self-consistent condition**, which commonly appears in mean-field approximation. For simplicity, we assume that the density of states $\mathcal{D}(E_F)$ around E_F is constant for energy. Then from

$$m = 2\mathcal{D}(E_F)\Delta\mu = \mathcal{D}(E_F)Um, \quad (6.37)$$

the condition $m \neq 0$ gives the criterion of appearance of nonzero m as

$$U\mathcal{D}(E_F) = 1. \quad (6.38)$$

We estimate the enhancement of kinetic energy by magnetization as we did in the electron gas. From the above condition we obtain

$$\mathcal{D}(E_F)(\Delta\mu)^2 = \frac{m^2}{4\mathcal{D}(E_F)}. \quad (6.39)$$

As in eq. (6.36), the decrease in the Coulomb repulsion energy by appearance of m is $-NUm^2/4$. Summing up of these gives

$$\Delta E = \frac{N}{4} \left[\frac{m^2}{\mathcal{D}(E_F)} - Um^2 \right]. \quad (6.40)$$

The condition $\Delta E < 0$ is

$$U\mathcal{D}(E_F) \geq 1, \quad (6.41)$$

which agrees with the criterion (6.38). This is called **Stoner condition**.

Roughly speaking, let E_w be the bandwidth and from $\mathcal{D}(E_F) \sim E_w^{-1}$, we can say that the Stoner condition means the ferromagnetism appears when the Coulomb interaction width U exceeds the bandwidth E_w . Because it is still a HF approximation, as in the case of electron gas, we have the problem of overestimation the stability of ferromagnetic state.

6.2.3 Susceptibility

Before going into the problem, we see the magnetic susceptibility given in the HF approximation. The magnetization M is expressed as

$$M = \frac{g\mu_B}{2} \sum_i [\langle n_{i\uparrow} \rangle - \langle n_{i\downarrow} \rangle] \frac{g\mu_B}{2} \sum_i n_{i-}. \quad (6.42)$$

The susceptibility χ per an atom is

$$\chi = \frac{M}{NB} = \frac{g\mu_B}{2} \frac{n_-}{B}. \quad (6.43)$$

Since the interaction energy of magnetic field and magnetic moment (Zeeman energy) is $-MB$, the energy of electrons in magnetic field is written as

$$E_B = E(0) + E_2 n_-^2 - N \frac{g\mu_B}{2} B n_-, \quad (6.44)$$

where n_- is small. And E_2 is

$$E_2 = \frac{1}{2} \frac{d^2(\Delta E)}{dn_-^2}, \quad (6.45)$$

where ΔE corresponds to ΔE in eq. (6.40).

In paramagnetic state, the coefficient of the term with the second order in M is positive in the GL theory. Then E_2 is also positive and n_- that minimizes E_B , gives the susceptibility. Namely,

$$\chi = \frac{(g\mu_B)^2 N}{4E_2}. \quad (6.46)$$

If we calculate E_2 from the HF approximation in eq. (6.40), we obtain

$$\chi = \left(\frac{g\mu_B}{2} \right)^2 \frac{\mathcal{D}(E_F)}{1 - U\mathcal{D}(E_F)} = \frac{\chi_{\text{Pauli(a)}}}{1 - U\mathcal{D}(E_F)}, \quad (6.47)$$

where $\chi_{\text{Pauli(a)}}$ is the Pauli paramagnetic susceptibility in eq. (3.8) per an atom.

In the HF approximation, when the system does not fulfill the Stoner condition, it keeps paramagnetism though as in eq. (6.47), the susceptibility is enhanced from the Pauli paramagnetic susceptibility by the factor $[1 - U\mathcal{D}(E_F)]^{-1}$. This is called **Stoner factor**.

Here from the identity of temperature expansion of the chemical potential when the system is strongly Fermi degenerated:

$$\mu = \mu_0 \left[1 - \frac{\pi^2}{6} \frac{d \log \mathcal{D}(\mu_0)}{d \log \mu_0} \left(\frac{k_B T}{\mu_0} \right)^2 + \dots \right], \quad (6.48)$$

the temperature variation of chemical potential $\delta\mu$ is written as

$$\delta\mu = -\frac{\pi^2 \mathcal{D}'_F}{6 \mathcal{D}_F} (k_B T)^2. \quad (6.49)$$

For simpler expression, $d\mathcal{D}(E)/dE|_{E=E_F}$ is simply written as \mathcal{D}'_F . To add this to $\Delta\mu$ in eq. (6.37) as correction, taking the second derivative by the energy is required. Hence we write

$$A = \frac{\pi^2}{6} \left(\frac{(\mathcal{D}'_F)^2}{\mathcal{D}_F} - \mathcal{D}''_F \right), \quad (6.50)$$

and the temperature dependence of susceptibility is written as

$$\chi = \left(\frac{g\mu_B}{2} \right)^2 \frac{\mathcal{D}(E_F)}{1 - U\mathcal{D}(E_F) + UA(k_B T)^2}. \quad (6.51)$$

The temperature that gives zero for the denominator is T_C , and by using this, we can write

$$\chi = \frac{C}{T^2 - T_C^2}. \quad (6.52)$$

This does not agree with the Curie-Weiss law, which is also observed in $3d$ transition metals with ferromagnetism. This indicates that the HF approximation has problems other than the quantitative problem we will see in the second next section.

6.3 Ferromagnetism in $3d$ transition metals

Before going into more realistic theories, we would like to have a look on experimental facts on the ferromagnetism in $3d$ metals. Those should be also the target of more realistic theory. We also see “tuning” of the exchange parameter gives a qualitative understanding of the experiments even within the HF approximation.

In the table below, the bulk parameters of the three elemental ferromagnetic metals are listed[6].

	structure /density (kgm^{-3})	lattice parameters (pm)	T_C (K)	M_S (MAm^{-1})	K_1 (kJm^{-3})	λ_S (10^{-6})	α	P (%)
Fe	bcc 7874	287	1044	1.71	48	-7	1.6	45
Co	hcp 8836	251 407 (fcc)	1388	1.45	530	-62	8.0	42
Ni	fcc 8902	352	628	0.49	-5	-34		44

Tab. 6.1 Bulk properties related to the ferromagnetism in Fe, Co, Ni. K_1 is density of anisotropic energy; λ_S spin diffusion length; α damping factor of spin resonance; P spin polarization. P is measured by the Andreev reflection at 4.2 K. The others are measured at room temperature. From [6].

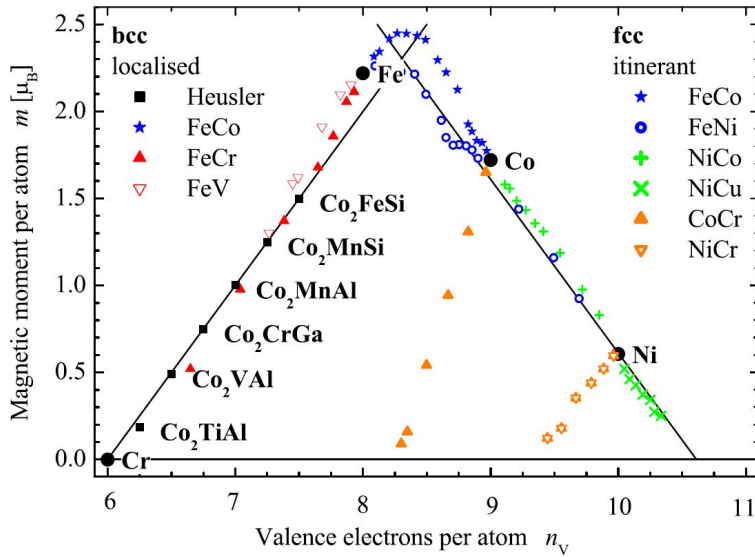


Fig. 6.2 Averaged spontaneous magnetic moment (in unit μ_B) is plotted as a function of averaged valence electron number (horizontal axis) for various 3d transition metals (elemental metals, and alloys). From [7]. Valence electron number 6 corresponds to Cr, 11 corresponds to Cu.

6.3.1 Slater-Pauling's curve

As shown above, among 3d transition metals, elemental metals that show ferromagnetism are Fe, Co, and Ni. The averaged valence electron numbers are 8, 9, 10 respectively. However, with making alloys with other 3d metals or Heusler alloys, which contains group III, or IV elements, we can synthesis metallic ferromagnets with the valence electron number from around 6 to about 10.5. Then we plot the spontaneous magnetization per an atom obtained from the saturated magnetization as a function of number of valence electrons. The data points align regularly as in Fig. 6.2. They are on the lines forming a triangle with Fe around the peak. And the edges of the triangle have gradients of ± 1 . This curve is called **Slater-Pauling' curve**.

In Fig. 6.2 the alloys plotted in the left region than Fe are mainly Heusler alloys. For Heusler alloys, the following relation is reported to hold[8]:

$$m_{\text{magnetization per atom in unit of } \mu_B} = Z - 24. \quad (6.53)$$

Relation like eq. (6.53) is called **Slater-Pauling law**.

6.3.2 Spin-band structure in Ni

This relation should come from the number of 3d electron spins in the open shell. Here, however, the “open shells” form an energy band and the electrons in it are itinerant. Then numerically calculated band structures are often used for the explanation of Slater-Pauling's curve. The band structure must have spin-dependence, that means the electron mutual interaction should be taken into account in some way. Many of them are the HF approximation, which is known to overestimate the exchange energy gain. But still, qualitative explanation of Slater-Pauling's curve is possible as follows.

Nickel (Ni) has fcc structure and T_C is comparatively low among the three elemental ferromagnets. Figure 6.3(a) shows the spin-dependent density of states calculated by the APW method (Appendix 12A)[9]. The 4s electron band has a widely spread density of states with low amplitudes. Conversely, the 3d electron band has a comparatively narrow distribution and has several high sharp peaks. A single spin subband of 4s electrons can accommodate a single electron per atom while that of 3d electrons can accommodate 5 electrons per atom. The bottom of 4s band is lower than that of 3d band. The position of E_F shown in Fig. 6.3(a) indicates that the 4s band as 0.6 electron, the 3d \uparrow band (the upper side in the figure. the major spin subband) has 5 electrons, the 3d \downarrow band has 5.4 electrons. 10 valence electrons are

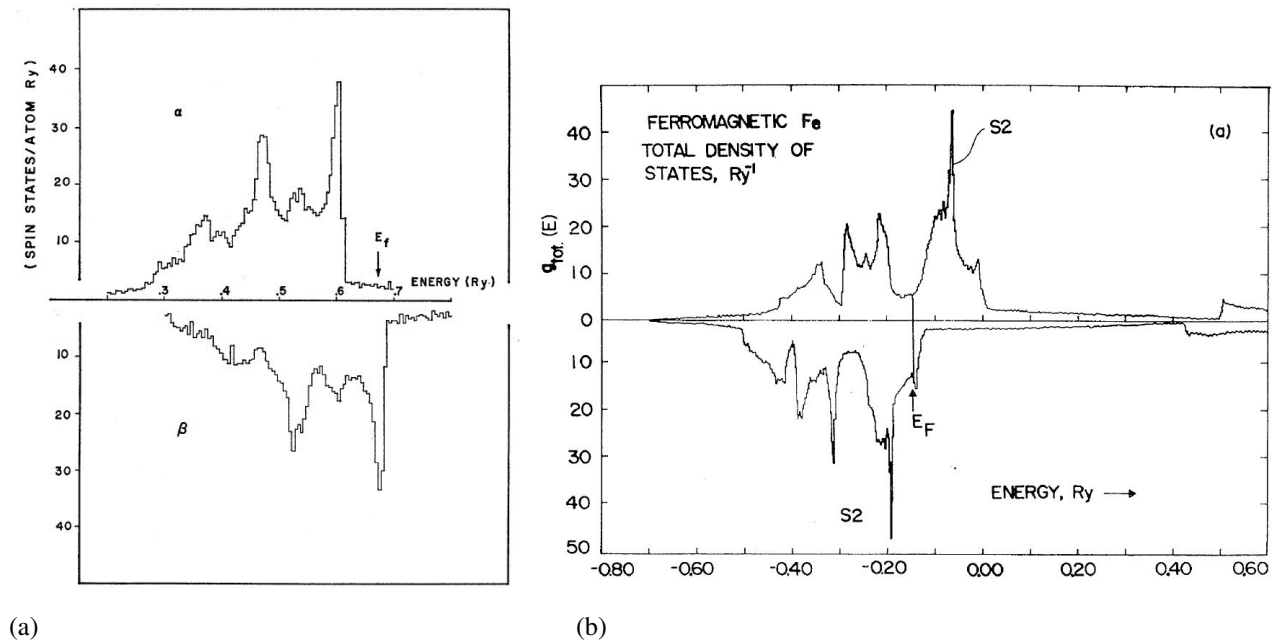


Fig. 6.3 Spin-dependent density of states in (a) Ni, (b) Fe, calculated by the APW method. (a) is from [9]. (b) is from [10].

in an atom in total. In total, the total spin for 0.6 electron remains, which fact explains the appearance of spontaneous magnetic moment with $0.6\mu_B$. As above, the non-integer spontaneous magnetic moment is explained by the coexistence of $4s$ band and $3d$ band and partial occupation of them by valence electrons.

In Ni-Cu alloys, the spontaneous magnetizations vanishes around 60% of Cu content. A Cu atom has 11 valence electrons, which is one more than Ni. Hence with increasing the Cu content, the extra one electron fills the vacant space of 0.6 electron in $3d \downarrow$ band. Just at 60%, the space is filled up and the spontaneous magnetization vanishes. Also, it is now clear that the gradient is -1 in Slater-Pauling's curve from Ni to Cu.

6.3.3 Spin band structure in Fe

Figure 6.3(b) shows the spin dependent density of states in bcc Fe calculated by the APW method. Though the shape of density of states resembles to that of Ni, there is a large difference in the position of E_F . The total electron number is 8 and the $4s$ band has 0.8 electron. Of the remaining 7.2 electrons, 4.7 electrons are in the major spin subband (the lower in the figure), 2.5 electrons are in the minor spin subband. The configuration brings about the spontaneous magnetization of $2.2\mu_B$.

The reason why the major spin subband does not have full 5 electrons can be explained in Fig. 6.3(b). In the case of Ni, E_F places above the $3d$ major spin subband while in the case of Fe, E_F hits a valley of the minor spin subband. In such a situation, a variation of electron number in the minor spin subband causes a large shift in the relative E_F position. The position of E_F in fixed energy space does not move largely. That means actually the whole band should move largely. Summing up the discussion, once E_F hits a valley of density of states, change of electron number is mostly absorbed by other subbands and E_F is locked to the valley. This makes it hard to increase the space (hole) in the minor spin subband. And the major spin subband still has some hole in it.

Alloying with Co increases the number of electrons, with which we can test the above hypothesis. When the Co concentration is low, the increasing electrons fill the major spin band, and the spontaneous magnetic moment increases with the Co concentration. At 30% where the major spin band is completely filled ($5 - 4.7 = 0.3$), the increasing electrons work in the direction of filling the holes in the minor spin band, and the number starts to decrease. For the same reason,

the moment decreases due to alloying with Cr, which reduces the number of electrons.

Appendix 12A: An example of band calculation (APW)

Numerical calculations that exceed the HF approximation are still not very common, and many theories used to explain the Slater-Pauling law are by (a bit-modified) HF approximation. Band calculation is often the basis for considering the electron correlation effect, so let us take a brief look at a type of calculation method here. Here we introduce APW (augmented plane wave) method, which is one of the techniques to find solutions of Kohn-Sham equation ^{*1}, for the details, refer to [11, 12] and the references therein.

Let us consider the Schrödinger equation of the state $\phi(\mathbf{r})$ in potential $V(\mathbf{r})$:

$$\mathcal{H}\phi(\mathbf{r}) = \left[-\frac{\hbar^2}{2m}\nabla^2 + V(\mathbf{r}) \right] \phi(\mathbf{r}) = E\phi(\mathbf{r}). \quad (12A.1)$$

As the potential, we consider one called Muffin-tin potential. Let r_c be the radius of Muffin-tins, which must be shorter than the half of the distance between neighboring atoms. Then the potential is described as (Fig. 12A.1)

$$V(\mathbf{r}) = \begin{cases} V_a(r) \text{ (spherical)} & (r < r_c) \\ V_o (= V_a(r_c): \text{const.}) & (r \geq r_c). \end{cases} \quad (12A.2)$$

As $V(\mathbf{r})$, Hartree potential, which corresponds to the direct integral in eq. (6.6), is adopted. That is

$$V_a(\mathbf{r}) = \sum_i \langle \phi_i(\mathbf{r}') | \frac{e^2}{|\mathbf{r} - \mathbf{r}'|} | \phi_i(\mathbf{r}') \rangle. \quad (12A.3)$$

And exchange potential which corresponds to the exchange integral is

$$V_{\text{ex}\uparrow} = -3e^2 \left(\frac{3}{4\pi} \right)^{1/3} \rho_{\uparrow}(\mathbf{r})^{1/3}. \quad (12A.4)$$

The above is from spin density function approximation. The above Hartree and exchange potentials are obtained from the eigen functions, which are the solutions of eq. (12A.1). Hence the equation constitutes the self-consistent equation.

Actual calculation is on the variational method. As the variation functions, we adopt

$$\Phi_{\text{vr}}(\mathbf{r}) = \begin{cases} \sum_{l,m} A_{lm} R_l(r) Y_l^m(\theta, \varphi) & r < r_c, \\ \sum_{n=0}^N B_n \exp[i(\mathbf{k} + \mathbf{K}_n) \cdot \mathbf{r}] & r > r_c. \end{cases} \quad (12A.5)$$

That is, inside the muffin-cup, wavefunctions have the same form for an isolated atom potential, and outside, the superpositions of plane waves. \mathbf{K}_n are inverse-lattice vectors.

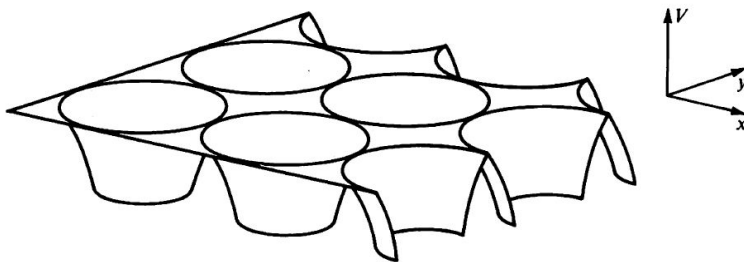


Fig. 12A.1 Schematic diagram of Muffin-tin potential. From [13].

^{*1} Though APW method was invented long before the Kohn-Sham equation, now it can be placed at such a position in the present understandings.

The wavenumber k is fixed and the variation is taken under the boundary condition of wavefunction Φ connection at $r = r_c$. Actually, the coefficients $\{B_n\}$ is determined for $\langle \Phi | \mathcal{H} | \Phi \rangle$ to take the extremals. N cannot be taken to infinity and the calculation is done within a finite number. Thus obtained Φ is used to calculate the potential and the procedure is continued to reach convergence. Then k is varied and the same procedure is repeated to obtain the band structure as we have seen in Sec. 6.3.

Appendix 12B: MateriApps

MateriApps (<https://ma.issp.u-tokyo.ac.jp/>) is a portal site for material science simulations operated in cooperation with the Institute for Solid State Physics CMS and others, and has information and download links for many related applications.



Among them, Quantum Espresso (<https://www.quantum-espresso.org/>) is an application that performs a wide range of calculations such as ground state calculation, DFT calculation, and quantum transport, and is characterized by being able to run on a PC.

References

- [1] A. A. Abrikosov. *Fundamentals of the Theory of Metals*. Dover Publications, 10 2017.
- [2] Alexander L. Fetter and John Dirk Walecka. *Quantum Theory of Many-Particle Systems (Dover Books on Physics)*. Dover Publications, 6 2003.
- [3] A. A. Abrikosov, L. P. Gorkov, and I. E. Dzyaloshinski. *Methods of Quantum Field Theory in Statistical Physics (Dover Books on Physics)*. Dover Publications, 10 1975.
- [4] Henrik Bruus and Karsten Flensberg. *Many-body Quantum Theory In Condensed Matter Physics: An Introduction (Oxford Graduate Texts)*. Oxford Univ Pr, 11 2004.
- [5] D. M. Ceperley and B. J. Alder. Ground state of the electron gas by a stochastic method. *Phys. Rev. Lett.*, Vol. 45, pp. 566–569, Aug 1980.
- [6] J. M. D. Coey. Materials for spin electronics. In *Lecture Notes in Physics*, pp. 277–297. Springer Berlin Heidelberg.
- [7] Benjamin Balke, Sabine Wurmehl, Gerhard H Fecher, Claudia Felser, and Jürgen Kübler. Rational design of new materials for spintronics: Co_2Fez ($z=\text{al, ga, si, ge}$). *Science and Technology of Advanced Materials*, Vol. 9, No. 1, p. 014102, January 2008.

- [8] I. Galanakis, P. H. Dederichs, and N. Papanikolaou. Slater-pauling behavior and origin of the half-metallicity of the full-heusler alloys. *Phys. Rev. B*, Vol. 66, p. 174429, Nov 2002.
- [9] John W. D. Connolly. Energy bands in ferromagnetic nickel. *Phys. Rev.*, Vol. 159, pp. 415–426, Jul 1967.
- [10] Rastko Maglic. Van hove singularity in the iron density of states. *Phys. Rev. Lett.*, Vol. 31, pp. 546–548, Aug 1973.
- [11] 和子望月, 直鈴木. 固体の電子状態と磁性. 大学教育出版, 7 2003.
- [12] Jorge Kohanoff. *Electronic Structure Calculations for Solids and Molecules*. Cambridge University Press, June 2006.
- [13] Walter A. Harrison. *Solid State Theory (Dover Books on Physics) (English Edition)*. Dover Publications, 4 2012.